Hindawi
Advances in Civil Engineering
Volume 2020, Article ID 7030425, 9 pages
https://doi.org/10.1155/2020/7030425

Review Article

Soil Fatigue from Induced Seismicity

Merissa L. Zuzulock,[1] **Oliver-Denzil S. Taylor**,[2] **and Norbert H. Maerz.**[3]

[1]*US Army Corps of Engineers, New York District, 5352 Delaware Ave., Joint Base MDL, NJ 08640, USA*
[2]*Geotechnical and Structures Laboratory, US Army Engineer Research and Development Center, 3909 Halls Ferry Road, Vicksburg, MS 39180, USA*
[3]*Missouri Science and Technology, Geological Engineering Department, 332 McNutt Hall, Missouri University of Science and Technology, Rolla, MO 65409-0410, USA*

Correspondence should be addressed to Merissa L. Zuzulock; merissa.l.zuzulock@usace.army.mil

Received 1 August 2019; Accepted 21 January 2020; Published 15 April 2020

Guest Editor: Tae-Hyung Kim

Induced seismicity and the effects on civil engineering systems are not completely understood and infrequently studied. One specific area that is not well known is soil fatigue which includes factors such as understanding the natural conditions of the subsurface as well as operational parameters under short duration impulse loads. With the increase of geoinduced seismic activity, soil fatigue becomes of greater concern to structures in the vicinity of this seismic load. The foundations of these structures can be affected by impulse loads which can ultimately cause failure. The lack of quantitative data puts the reliability of these civil engineering systems at risk as they are not fully evaluated to determine if they are functioning as they are intended in the environments they are designed to support.

1. Introduction

Soil fatigue occurs prior to failure which makes it difficult to define as it is determined based on the acceptable level of risk the system can sustain. Determining factors for failure are usually based on social benefits and/or economic judgments that are difficult to quantify [1]. For purposes of this paper, soil fatigue can be defined as the magnitude of strain that a material can endure for a given number of cycles until a point of maximum strain where the soil begins to weaken. Similar to fatigue for other engineering structures bridges, roads, metals, etc., it is further defined as losing strength over time without catastrophic failure. However, such fatigue can ultimately lead to failure if left unchecked as it will continue to grow as the amount of applied impact load increases.

The increase in geoengineered induced seismicity has created concerns for several civil engineering systems such as dams and levees. To date, the study of impacts from induced seismicity has been rare with indeterminate conclusions with significant volumes of research into the causality of geoengineered induced seismicity. However, little research has been completed into the accumulative effects of frequent colocated events as a single geoengineered event is assumed to be minor to cause any damage or degradation of the overlying soil structure [2–4].

There is an abundance of literature regarding the study of single seismic event loading [5, 6], as well as the behavior of partially saturated soils under cyclic loading [7, 8]. However, these studies assume that the loading from geoengineered induced seismicity can be treated as isolated single events where the soil structure can fully recover before the next loading. Induced seismicity records from throughout the Central United States illustrate regions of close spaciotemporal small magnitude events, i.e., swarms, wherein any isolated event would typically be considered insufficient to cause any surficial expression of damage [2, 3]. However, the cumulative effect of the close spaciotemporal swarms is not well understood and can potentially cause a fatigue condition within the soil.

To study soil fatigue, this paper presents a modified damage equation to account for degradation of soil structure as a result of low frequency impulsive loading, i.e., a proxy for spaciotemporal small magnitude events.

2. Geoengineered Activity and Induced Seismicity

Concerns regarding induced seismic activity have increased exponentially since 2009 due to the increase in the number of induced earthquakes magnitude (M) of 3.0 or larger [9]. Overall, the number of earthquakes in the central United States, M3.0 or larger, increased showing an average of around 300 earthquakes per year from 2009 to January 2016 [10]. In 2009 there were approximately 29 M3.0 or larger earthquakes with a large increase between 2009 and 2016 increasing to 330 M3.0 or larger earthquakes per year in 2016 [9].

A study was conducted in the western boundary of the stable Canadian craton using the three largest ground motion events: M4.0 and M4.2 near Fort St. John (FSJ), British Columbia, and an M3.9 in close proximity to the Rocky Mountain House (RMH) in Alberta that occurred between 30 July 2014 and 9 August 2014. The location selected for the study is a low-to-moderate seismic region which poses a large risk to infrastructure as it may not have been designed to resist strong ground motions because of the low probability of naturally occurring strong ground motions in the area [11]. In early investigations, the authors determined that moderate induced events (M4-5) could damage nearby infrastructure due to the shallow focal depth that can result in concentrated strong ground motions. The study was conducted using a sparse seismograph network to record the two events at FSJ, located anywhere from 15 km to several hundred km away. The recordings from these three events of M~4 were then used to examine their ground motions along with their weakening with distance. When this study was conducted, the M4.2 event was the largest event related to hydraulic fracturing in the world. The two events at FSJ were determined through intesity assessments, ground motion characteristics, and focal depth estimations to be likely induced from hydraulic fracturing. They occurred at shallow (2–5 km) depths that could be felt at distances over 200 km at a maximum intensity of M4.2 for the largest event. The third event at RMH was M3.9 and was the strongest event in Alberta in more than a decade. The focal depths were determined to be between 4 km and 8 km and the area shows no records of oil and gas drilling in recent years. The RMH event was felt by nearby residents and had reported intensity of M4-5 and caused a shutdown of a nearby gas plant and a power outage that lasted for many hours. All of these events were widely felt and had the potential to cause damage to infrastructure.

A study in Oklahoma [9] shows a definite increase in earthquakes beginning in 2009 with a steep increase from 2014 to 2015. Oklahoma does have a history of seismicity but recent studies show that it is highly unlikely that these are caused through natural fluctuations in the rates of earthquakes. Central Oklahoma has created cause for concern especially since it has had more than 60 earthquakes at M4.0 to M4.8 starting in 2009 to the middle of 2016. There were larger events recorded in the same timeline that are currently under investigation due to the potential damaging effects of the seismic activity associated with the magnitude. One major earthquake was in Prague, Oklahoma, registered at M5.6 and was recorded [12] in November 2011. It destroyed 14 homes, injured two people, and buckled some parts of the highway and 17 other states could feel the tremble [13]. The largest earthquake documented was in Pawnee, Oklahoma, which was recorded at M5.8 causing substantial damage to infrastructure [9]. The M5.8 earthquake in Pawnee, OK, in September 2016, was the biggest recorded in the state and could possibly be related to wastewater injection.

There is statistical data that supports this conceptual model that shows the seismic activity linked to the distance between the basement and the injection point. This data provides regulators with information on how pore pressure develops through the knowledge of existing faults and ambient stress levels [14]. The study included a gas extraction process as studied in Groningen, The Netherlands. The process established for gas production compacts the reservoir that causes the build-up of stress along faults. Because of preexisting offsets, compartment reservoirs that have varying compaction levels meet along the faults. The compaction differences can increase the built-up stress at the faults which can in turn increase the occurrence of earthquakes [14]. Through subsidence measurements used to calibrate reservoir compaction in models, it identified seismicity concentrated in locations of high subsidence and compaction. These induced events are recorded after a reduced reservoir pore pressure by ~10 MPa with the outcome of an increase in rock stress that is of similar magnitude [14]. This conflicts with observations in Oklahoma that shows pressure disturbances of ~0.1 MPa initiating earthquakes. This shows that the crust is critically stressed and has a subset of faults that are near failure that can cause activation through a small amount of disturbance of stress [14].

In both of these activities, location and timing of the induced seismic activity are controlled by the distribution of space and the make-up of preexisting faults with existing stress conditions prior to subsurface work [14]. The current assumption regarding the size of induced events is that failures from induced activity are confined within the volume of rock that is affected by changes in stress of fluid pressure. However, recent studies by Van der Elst et al. [15] and Galis et al. [16] contradict this assumption and show that earthquakes induced from human activity could potentially fail outside of the volume that is affected. So that size of the induced earthquake can be manipulated through preexisting natural fluctuations of stress along the fault similar to natural events [14]. In either case, evidence suggests the need to understand preexisting faults as well as their stress level. Mitigation measures need to include both operational parameters, i.e., volume produced and volume injected, but must also include knowledge of the status of faults within the subsurface. This can be identified through hydromechanical modeling, operation parameters calibrated by independent measures through the use of InSAR to identify surface deformations [14].

A study was conducted by Zalachoris and Rathje [17] to develop ground motion models (GMMs) for small to moderate sized, potentially induced earthquake events in Texas, Oklahoma, and Kansas. The team created a database

with events with epicenters in those specific locations through the use of the Incorporated Research Institutions for Seismology (IRIS), 2018. Events that had at least 3 ground motions and at magnitudes that were greater than 3.0 were used for this effort which included 4,528 ground motions that were recorded during 376 events with hypocentral distances at less than 500 km. In an effort to quantify site amplifications, the team used the P-wave seismogram method that uses theoretical wave propagation considerations as well as recordings from seismic stations to estimate the VS30 at 251 seismic station locations within the defined area. In addition, the team investigated the relationship between geologic conditions and VS30 estimates at each location. This new model predicts smaller ground motions than other models and predicts an increase in ground motions at hypocentral distances less than or equal to 20 km. The newly scaled VS30 was determined to be weaker than other models and less amplified at VS30 <600 m/s [17]. It should be noted that there is an abundance of research into the source initiation and spectral characteristics of induced seismicity (see, e.g., [18–20]).

There have been several notable studies investigating the seismic vulnerability of structures to induced seismicity (see, e.g., [21–25]). These studies illustrate that there exists the potential for structural susceptibility for moderate to slight damage from induced seismicity. While the severity of the potential damage to structures from induced seismic events may not be as significant as HAZUS models based on the New Madrid Seismic Zone, these results clearly indicate that the potential damage is not insignificant. To further illustrate damage potential on structures from the increase in seismicity in parts of the central United States, a recent study by Liu et al. [25] identified that nonstructural components of structures have the potential to sustain damage from induced events as well as increased risk towards potential building collapse. In particular, Chase et al. [22] indicated that in the case of light-frame wood structures the structural damage and fragility did not seem to be accumulating with sequential seismic loadings. Liu et al. [25] calculated life-safety risk from the USGS 2016 one-year seismic hazard model as well as the fragility curves that are defined in the 2015 NEHRP (National Earthquake Reduction Program) Provisions. These results indicate that life-safety risks for modern buildings, in areas that are close to active induced seismic zones, have the potential to exceed the risks calculated from the 2015 NEHRP provisions' report that considers natural seismicity alone [25]. Therefore, if nonstructural components can sustain damage and increase the potential risk of structural collapse from induced seismicity, then the logical question is as follows: "Can the fatigue of the subsurface yield similar increased risk?" Moreover, do sequential induced seismic events have an accumulative effect on the fragility or fatigue of the subsurface?

3. Laboratory Observations of Soil Fatigue for Impulsive versus Cyclic Loading

To determine the reliability of a system, an object is assessed to determine failure which is the lack of ability of a system to function normally under the same specified conditions for the same amount of time [1]. In the case of soil mechanics, the point of failure is determined via an ultimate, or peak, failure condition, typically occurring when the strains exceed between 2% and 5%. However, failure of the soil structure can occur at a significantly lower strain [26, 27]. This loss of soil structure stiffness can result in small-scale collapses, i.e., small-strain compression, yielding, or settlement, as the soil element transitions to the next quasi-stable soil structure. If the excitation sources, e.g., impulses from pile driving, occur at a rate where the soil structure is continually forced to transition to the next quasi-stable state, the summation of the small-strain compression can cause superstructures, e.g., buildings and infrastructure, to exceed allowable design tolerances without causing an ultimate failure, e.g., structural collapse. This behavior defines the soil fatigue process. As subjective as failure is, soil fatigue is as well and far more difficult to identify as the experience which is usually known as the factor of safety is unknown [1]. This makes it difficult to quantify soil fatigue from close proximity spaciotemporal small magnitude events.

In a study conducted by the Engineering Research and Development Center, Geotechnical and Structures Laboratory (ERDC-GSL), laboratory tests were conducted to show the difference in dynamic behavior of near-surface partially saturated sand in reference to the potential for liquefaction from both cyclic and impulse loadings [28]. The outcome of these tests identifying the effects of near-surface soils with equivalent sinusoidal loads does not show the same strains as impulse loads to represent seismic waveforms that are irregular [28]. The 0.3% axial strain yield threshold is used based on a study conducted by [29] to identify significant limiting strain at the beginning of movement from pile strikes that began around 0.3% ε_{da}. The study consisted of a series of cyclic tests shown in Table 1 with the number of cycles needed to attain a certain double amplitude axial strain, ε_{da}, as shown in Figure 1. The results suggest that an exponential increase in the rate of strain starts to occur at around 0.3% ε_{da}, which is prior to the ultimate failure threshold of 5% ε_{da}. Additionally, it was observed that 47% of the completed tests reached 0.1% ε_{da} within the first cycle which suggests that the use of 0.1% as a yield initiation threshold would be overly conservative. Further tests identified that the capacity at 0.3% ε_{da} is about half of the difference of 0.1% and 5% ε_{da} and is about the mean of the distribution of the capacity-strain threshold, as shown in Figure 1 [29]. Therefore, a yield initiation, or fatigue, threshold of 0.3% ε_{da} as the maximum allowable fatigue stain for saturated dynamic loading is justified.

Taylor et al. [28] identify changes in dynamic behavior of near-surface partially saturated sand illustrating the strain potential from comparable cyclic and impulse loading wherein ten partially drained triaxial impulse and cyclic tests were conducted on poorly graded medium-fine beach sand with 24% saturation with a confinement of 10 kPa. An ultimate failure criterion of 2.5% axial strain was imposed based on samples tested through triaxial testing for a qualitative comparison of the loading requirements needed to cause an ultimate failure condition; see Figure 2 and Table 2 [28]. The test results showed no signs of liquefaction

Table 1: Summary of cyclic triaxial tests results from [29].

Test no.	N	CSR 0.1% ε_{da}	NEC	N	CSR 0.3% ε_{da}	NEC	N	CSR 1% ε_{da}	NEC	N	CSR 3% ε_{da}	NEC	N	CSR 5% ε_{da}	NEC
CYC-10-56	13	0.147	0.0012	18	0.146	0.0017	20	0.144	0.0019	22	0.138	0.0021	23	0.139	0.0021
CYC-10-57	69	0.118	0.0035	79	0.117	0.0039	81	0.117	0.004	83	0.116	0.0042	84	0.116	0.0042
CYC-10-58	2	0.175	0.0005	6	0.17	0.0017	7	0.164	0.0022	8	0.157	0.0024	9	0.151	0.0026
CYC-05-10	1	0.193	0.0008	2	0.183	0.0021	3	0.156	0.0041	3	0.156	0.0041	4	0.138	0.0053
CYC-05-11	9	0.15	0.001	15	0.147	0.0024	16	0.143	0.0037	16	0.143	0.0037	17	0.14	0.0037
CYC-05-12	1	0.179	0.0004	5	0.177	0.0016	6	0.169	0.0027	7	0.156	0.0044	7	0.156	0.0044
CYC-05-13	53	0.132	0.0029	63	0.131	0.0036	64	0.131	0.004	65	0.13	0.0046	65	0.13	0.0046
CYC-05-14	1	0.195	0.0006	2	0.192	0.0013	3	0.171	0.0033	4	0.149	0.0055	4	0.149	0.0055
CYC-05-16	34	0.121	0.0014	43	0.12	0.0019	45	0.119	0.0022	45	0.119	0.0022	46	0.118	0.0023
CYC-05-32	1	0.176	0.0004	6	0.175	0.002	8	0.167	0.0032	9	0.159	0.0038	9	0.159	0.0038
CYC-05-33	10	0.139	0.0011	22	0.138	0.0025	24	0.136	0.0031	25	0.134	0.0034	25	0.134	0.0034
CYC-05-34	12	0.13	0.001	27	0.129	0.0024	29	0.127	0.0028	30	0.126	0.003	31	0.124	0.0032
CYC-05-35	15	0.12	0.001	35	0.119	0.0024	38	0.117	0.0028	39	0.116	0.003	40	0.115	0.0032
CYC-05-36	21	0.11	0.001	74	0.109	0.0033	78	0.108	0.0037	80	0.107	0.004	80	0.107	0.004
CYC-05-43	1	0.157	0.0003	5	0.156	0.0013	8	0.15	0.0026	9	0.145	0.0029	9	0.145	0.0029
CYC-06-19	5	0.149	0.0005	13	0.147	0.0013	15	0.144	0.0015	16	0.14	0.0015	17	0.137	0.0015
CYC-06-20	1	0.168	0.0002	7	0.167	0.0013	9	0.163	0.0018	10	0.159	0.002	11	0.152	0.002
CYC-06-21	7	0.13	0.0004	27	0.129	0.0014	30	0.127	0.0016	31	0.126	0.0016	32	0.124	0.0017
CYC-06-28	10	0.139	0.0007	21	0.138	0.0015	23	0.137	0.0017	24	0.135	0.0017	25	0.133	0.0017
CYC_10_82	57	0.139	0.0024	85	0.139	0.0029	87	0.139	0.0031	89	0.139	0.0032	90	0.139	0.0032
CYC_10_68	26	0.15	0.0014	34	0.149	0.002	36	0.15	0.0023	38	0.149	0.0024	38	0.149	0.0024
CYC_10_63	10	0.18	0.0011	18	0.18	0.0021	20	0.18	0.0026	21	0.179	0.0029	21	0.179	0.0029
CYC_10_60	1	0.208	0.0003	7	0.209	0.0016	9	0.208	0.0023	10	0.207	0.0027	10	0.207	0.0027
CYC_10_66	1	0.228	0.0006	2	0.227	0.0013	3	0.226	0.0026	4	0.225	0.0039	4	0.225	0.0039
CYC_10_101	1	0.297	0.0013	1	0.297	0.0013	2	0.291	0.0052	2	0.291	0.0052	3	0.281	0.0069
CYC_10_59	1	0.207	0.0003	7	0.207	0.0017	9	0.204	0.0025	10	0.2	0.0027	11	0.195	0.0027
CYC_10_79	71	0.137	0.002	82	0.137	0.0025	85	0.137	0.0027	87	0.137	0.0028	88	0.137	0.0029
CYC_10_67	42	0.149	0.0019	52	0.148	0.0026	54	0.148	0.0028	56	0.146	0.0029	57	0.146	0.003
CYC_10_70	38	0.149	0.002	46	0.148	0.0025	48	0.148	0.0028	50	0.146	0.0029	52	0.145	0.003
CYC_10_88	23	0.156	0.0031	34	0.158	0.0041	35	0.158	0.0044	36	0.158	0.0049	37	0.157	0.0056
CYC_10_53	7	0.187	0.0008	14	0.186	0.0017	17	0.183	0.0021	19	0.179	0.0023	20	0.177	0.0023
CYC_10_89	8	0.172	0.0012	19	0.178	0.0029	20	0.178	0.0032	21	0.178	0.0038	22	0.178	0.0047
CYC_10_52	5	0.207	0.0009	10	0.205	0.0018	12	0.203	0.0023	14	0.198	0.0024	15	0.194	0.0025
CYC_10_51	3	0.225	0.0008	8	0.225	0.0021	10	0.221	0.0029	11	0.217	0.003	12	0.211	0.0031
CYC_10_99	1	0.225	0.0003	8	0.224	0.0021	10	0.219	0.0029	11	0.214	0.0031	13	0.209	0.0034
CYC_10_54	1	0.244	0.0003	8	0.241	0.0023	10	0.238	0.003	11	0.234	0.0032	12	0.229	0.0032
CYC_10_100	3	0.256	0.0008	8	0.254	0.0023	10	0.249	0.0032	11	0.244	0.0034	12	0.239	0.0356
CYC_10_98	1	0.251	0.0006	3	0.244	0.0021	4	0.234	0.0029	5	0.218	0.0032	5	0.218	0.0032
CYC_10_95	1	0.284	0.0012	1	0.284	0.0012	4	0.278	0.0035	6	0.262	0.0044	7	0.253	0.0046
CYC_10_97	1	0.291	0.0009	2	0.288	0.0012	4	0.273	0.0038	5	0.256	0.0042	5	0.256	0.0042
CYC_10_71	92	0.148	0.0039	104	0.148	0.0045	107	0.147	0.0046	110	0.146	0.0047	111	0.146	0.0048
CYC_10_62	5	0.201	0.0008	11	0.197	0.0019	13	0.192	0.0022	15	0.183	0.0024	16	0.18	0.0026
CYC_10_65	1	0.23	0.0004	4	0.226	0.0015	6	0.214	0.0022	8	0.197	0.0026	9	0.192	0.003
CYC-05-49	1	0.186	0.0003	14	0.186	0.0021	19	0.184	0.0031	23	0.181	0.0038	25	0.18	0.0041
CYC-05-48	1	0.204	0.0004	7	0.204	0.0019	10	0.202	0.0029	14	0.198	0.0042	17	0.196	0.005
CYC-05-47	1	0.22	0.0006	3	0.218	0.0016	5	0.215	0.0027	9	0.211	0.0043	11	0.208	0.0049
CYC-05-46	1	0.24	0.0008	2	0.233	0.0014	4	0.233	0.0027	7	0.228	0.0043	9	0.225	0.0051
CYC-06-01	1	0.191	0.0005	5	0.192	0.0017	9	0.189	0.0031	12	0.181	0.004	13	0.177	0.0041
CYC-06-02	1	0.196	0.0002	10	0.195	0.0016	13	0.193	0.0029	15	0.19	0.0036	16	0.186	0.0038
CYC-06-03	1	0.214	0.0004	5	0.213	0.0015	8	0.21	0.0028	10	0.204	0.0037	11	0.199	0.0039
CYC-06-04	1	0.233	0.0005	3	0.232	0.0014	6	0.225	0.0033	8	0.215	0.0042	9	0.207	0.0043
CYC-06-10	1	0.272	0.0004	13	0.275	0.004	24	0.274	0.0087	30	0.272	0.0125	32	0.27	0.0134
CYC-06-11	1	0.313	0.0007	2	0.313	0.0013	10	0.311	0.0071	14	0.308	0.0112	16	0.304	0.0129
CYC-06-12	1	0.294	0.0006	6	0.295	0.003	15	0.293	0.0086	20	0.29	0.0131	22	0.281	0.0146

or symptoms of uncontrolled straining as observed in saturated conditions, e.g., Taylor [29]; however, the impulse tests did reach the 2.5% straining threshold where an equivalent cyclic load did not. All of the impulse load tests exceeded the failure criteria of 2.5% ε_a between 9 and 19 cycles with an average of 12 cycles to failure. Only three of the cyclic test reached the 2.5% failure criteria with an average of 100 cycles to failure. This study identifies the need to

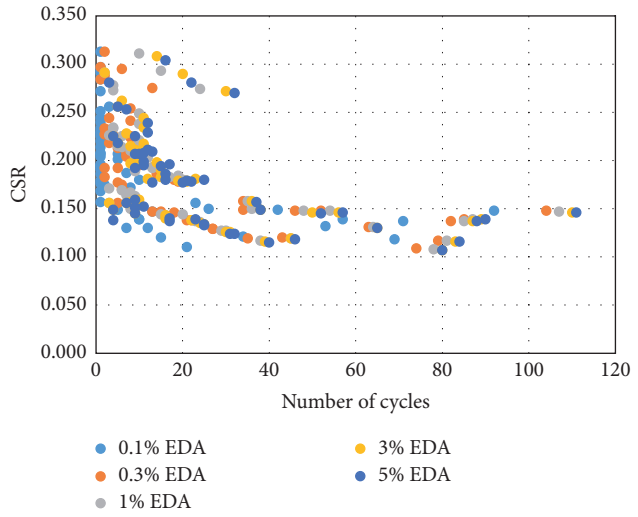

Figure 1: Data from Taylor [29] comparing number of cycles to initiate varying strains.

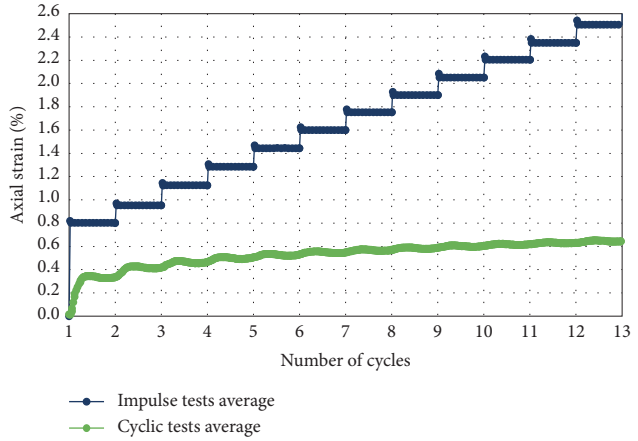

Figure 2: Comparison of impulse loading and uniform 1 Hz cyclic loading.

study cyclic and impulse loads with respect to near-surface seismic resistance. As shown by the data, cyclic loads, the increase in axial strain is nonlinear and has a logarithmic trend with a low number of cycles followed by a large increase at 50 cycles which identifies the potential for softening of the soil; however, this is not enough to reach liquefaction. On the other hand, impulse loads showed the increase in strain to be linear after an initial loading spike which identifies a constant strain [28].

4. Determining Damage Potential from Soil Fatigue

It is feasible through innovative processes to determine damage from soil fatigue that will allow engineers to identify when the system is not functioning as it should. Most studies are focused on the effects of cyclic soil degradation on soil strengths but neglect including potential damage from impulse loads. In addition, the damage accumulation effects from earthquake swarm events are largely unknown. Newmark's [30] sliding block analysis touches on this concept but focuses on a single earthquake with a distinct number of times the acceleration exceeds the threshold. The focus of this paper is to consider multiple events in close proximity where each event has a single time the acceleration exceeds a threshold value. Based on Taylor et al. [28], it is important that cyclic and impulse loading tests are treated differently so equation (1) is introduced to identify a more accurate picture of liquefaction from induced seismic events. To consider the seismic design of a structure in this paper, a conceptual model is provided to analyze the equations presented in this paper.

The pseudostatic slope stability method is a commonly used procedure to determine slope stability under seismic loading that was introduced by Seed [31]. It was further improved by Bray and Travasarou [32, 33] to better rationalize the identification of the seismic coefficient used in the analysis. This method uses a probabilistic seismic slope displacement model to determine slope stability under seismic loading. It uses the yield coefficient (k_y), the initial fundamental time period of the sliding mass (T_s), along with a degraded time period of spectral acceleration $(S_a)1.5T_s$, (M) being the moment magnitude of the earthquake, and ε being the normal distributed random variable. Equation (1) represents the number of nonzero seismic displacement (D) events:

$$\begin{aligned}\ln(D) = {} & -1.10 - 2.83 \ln\left(k_y\right) - 0.333\left(\ln\left(k_y\right)^2\right) \\ & + 0.566\ln\left(k_y\right)\ln\left(S_a(0.39)\right) + 3.04\ln\left(S_a(1.5T_s)\right) \\ & - 0.244\left(\ln\left(S_a(1.5T_s)\right)\right)^2 + 1.50T_s + 0.278 \\ & \cdot (M - 7) \pm \varepsilon.\end{aligned} \tag{1}$$

The example presented in this paper is created as an example for potential settlement from earthquake swarm events on a standard office building. The below slope stability analysis was completed through the use of the Seismic Landslide Movement Modeled using Earthquake Records (SLAMMER) program created for the USGS [34]. The program is used to analyze permanent deformations of slopes to identify how they behave during an earthquake. The Bray and Travasarou [32] method was used for this analysis with the use of existing data incorporated into the SLAMMER system as well as assumptions that were used to calculate displacement. Using the data included in the SLAMMER system, shown in Figures 3 and 4, the below record was used as a sample product for the calculations used in the Bray and Travasarou flexible (coupled) method with a modification of the earthquake magnitude from M7 to M4 to represent the potential for damage at small magnitudes [34].

The Bray and Travasarou flexible coupled method was selected to estimate permanent displacement from a single deterministic event or the probability of exceeding specific permanent displacements [34]. The flexible analysis estimates the nonzero displacement as well as the probability of

Table 2: Test results from equivalent cyclic and impulse loading [4].

Specimen	Test program	Initial water content (%)	Posttest water content				Number of cycles to 2.5% ε_a
			Top (%)	Middle (%)	Bottom (%)	Average (%)	
SP200-I-1	Impulse	5.53	4.20	6.24	7.63	6.02	13
SP200-I-2	Impulse	5.51	4.87	5.89	6.83	5.86	11
SP200-I-3	Impulse	5.55	4.77	5.77	7.77	6.10	16
SP200-I-4	Impulse	5.54	4.69	5.85	9.07	6.54	14
SP200-I-5	Impulse	5.56	4.75	5.85	6.92	5.84	11
SP200-I-6	Impulse	5.55	4.37	5.25	7.87	5.83	15
SP200-I-7	Impulse	5.37	4.95	5.89	7.49	6.11	16
SP200-I-8	Impulse	5.59	4.36	5.33	7.25	5.65	9
SP200-I-9	Impulse	5.55	4.86	5.63	7.99	6.16	10
SP200-I-10	Impulse	5.58	4.41	6.56	8.15	6.37	11
Average	*Impulse*	*5.53*	*4.62*	*5.83*	*7.70*	*6.05*	*12*
SP200-C-1	Cyclic	5.53	4.91	6.17	6.87	5.98	96
SP200-C-2	Cyclic	5.71	4.14	5.62	7.05	5.60	n/a
SP200-C-3	Cyclic	5.68	4.59	6.19	7.50	6.09	n/a
SP200-C-4	Cyclic	5.48	4.47	5.77	6.87	5.70	n/a
SP200-C-5	Cyclic	5.59	5.54	8.04	9.40	7.66	n/a
SP200-C-6	Cyclic	5.59	4.65	5.17	6.25	5.36	n/a
SP200-C-7	Cyclic	5.58	4.52	5.51	7.35	5.79	n/a
SP200-C-8	Cyclic	5.54	4.38	5.89	7.03	5.77	n/a
SP200-C-9	Cyclic	5.57	4.60	5.07	7.04	5.57	74
SP200-C-10	Cyclic	5.53	4.63	4.89	7.29	5.60	63
Average	*Cyclic*	*5.58*	*4.64*	*5.83*	*7.27*	*5.91*	*n/a*

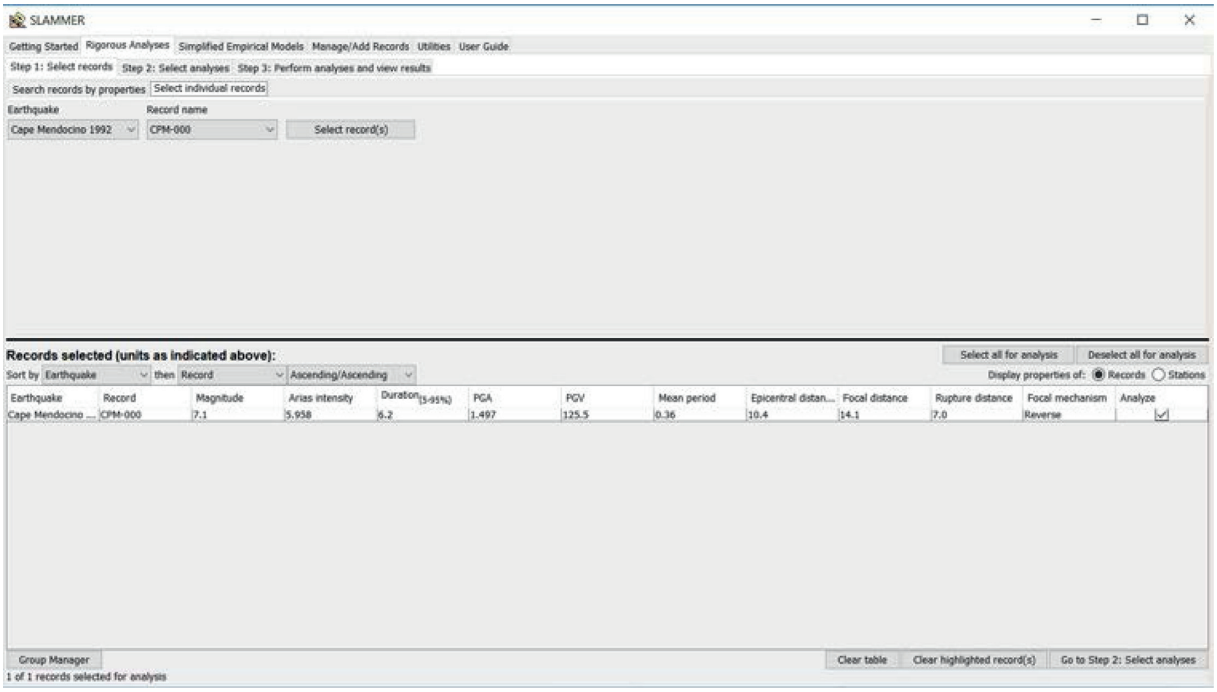

Figure 3: Soil properties from SLAMMER.

zero displacement. Figure 5 shows the correlation of the yield coefficient to the median displacement from data shown in Table 3. The data shows little to no displacement based on the above parameters.

In an effort to identify soil fatigue from earthquake swarms and show that induced seismic events have shorter dominating peak accelerations as well as shorter durations (2) was modified from Allotey and Nagger [35] damage equation to replace cyclic loading with impulse loading as well as adding an additional nonlinear stress dependent variable:

$$D = D\left(N, N_f(S)\right) = \left(N_f(S)\right)^{\Theta(S)}, \tag{2}$$

where D is the constant stress-controlled loading, fatigue damage function that is assumed to be a single valued deterministic figure that is nondimensional, and nondecreasing part of the stress ratio under a given number of

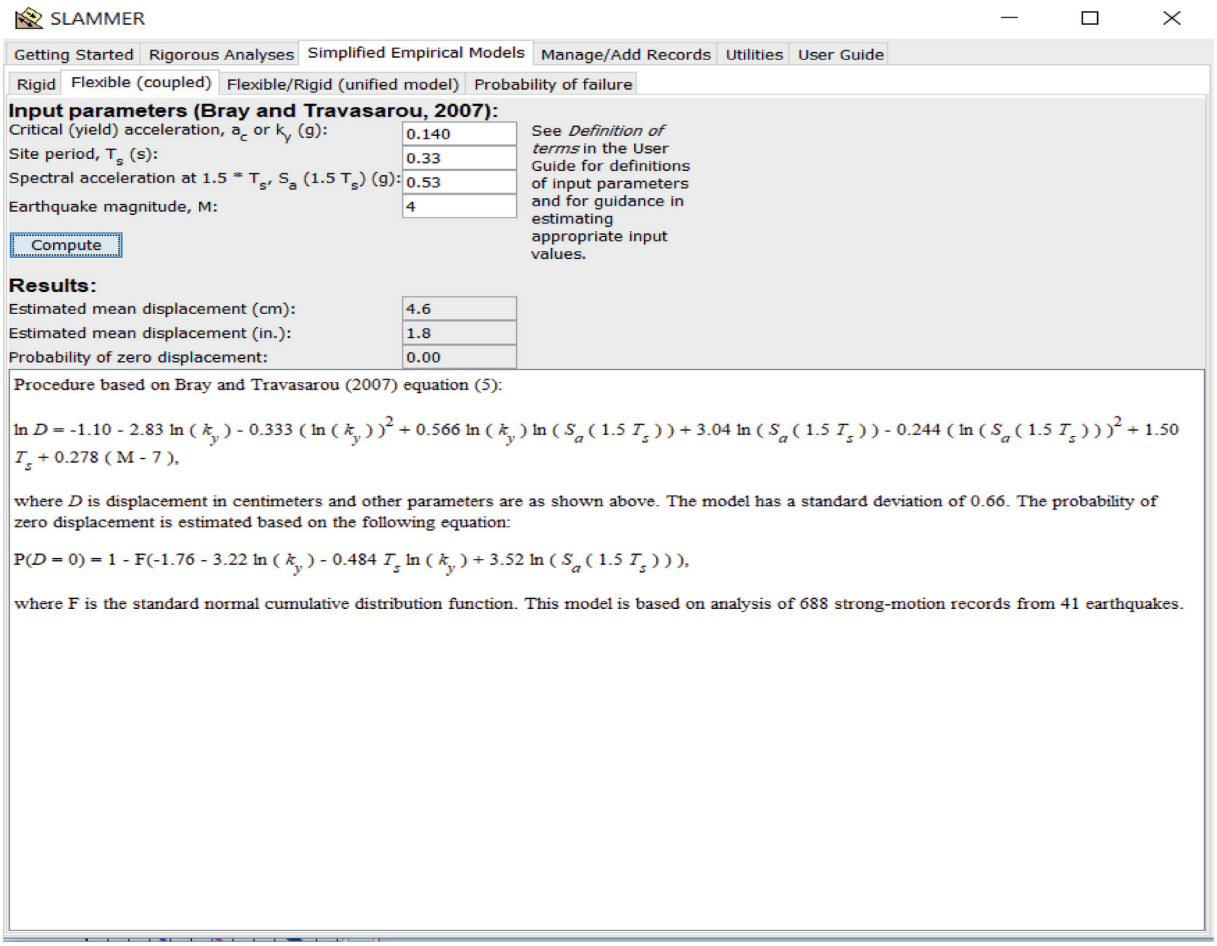

Figure 4: Bray and Travasarou [32] displacement analysis from SLAMMER.

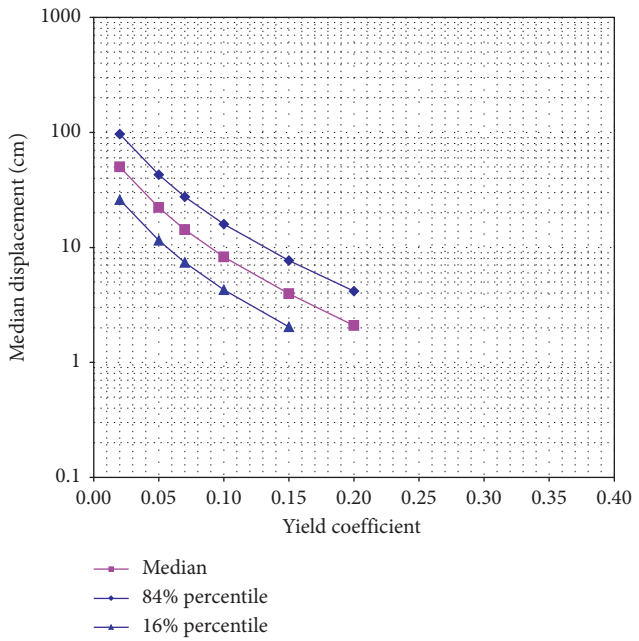

Figure 5: Bray and Travasarou [32] comparison of displacement to yield coefficient.

Table 3: Bray and Travasarou dependence on k_y [32].

Dependence on k_y	P (D = "0")	D (cm)	D_{median} (cm)	D_1 (cm)	D_3 (cm)
0.020	0.00	50.1	50.1	96.5	26.0
0.05	0.00	22.2	22.2	42.7	11.5
0.07	0.00	14.3	14.3	27.5	7.4
0.1	0.00	8.3	8.3	15.9	4.3
0.15	0.01	4.0	4.0	7.7	2.0
0.2	0.07	2.2	2.1	4.2	0.9
0.3	0.47	0.9	0.3	1.3	<1
0.4	0.82	0.4	<1	0.2	<1

cycles. N is the current number of cycles elapsed at the stress ratio S and N_f (S) is the number of cycles of the stress ratio, S, to reach failure. Failure is defined as soil fatigue which is determined to be the magnitude of strain that a material can endure for a given number of cycles until a point of maximum strain where the soil no longer functions as intended. The stress ratio, S, is the initial mean effective confining stress and Θ is a nonlinear function with loading cycles that is a stress dependent variable in the applied stress (CSR) and confining pressure. As the stress levels vary, the damage rate

Table 4: Changes in D.

Number of cycles to failure (N)	ε_{da}	S	$\Theta(S)$	D
13	0.1	0.147	0.0735	1.048752
18	0.3	0.146	0.073	1.073081
20	1	0.144	0.072	1.079136
22	3	0.138	0.069	1.079640
23	5	0.139	0.0695	1.084126

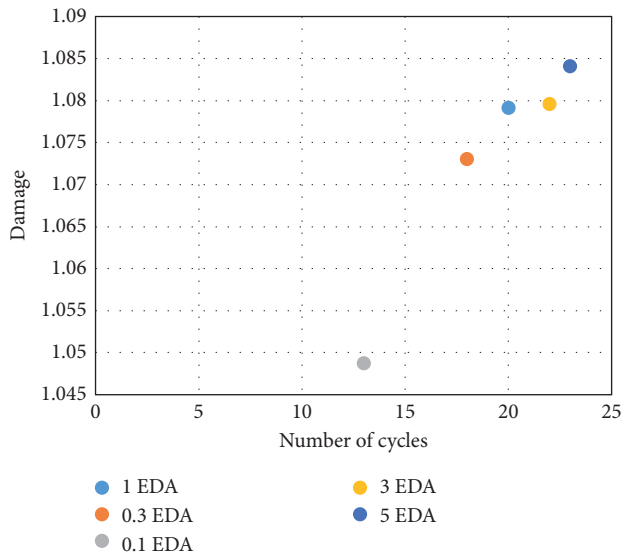

Figure 6: Comparison of change in D to strain.

changes; depending on the sequence of loading, the life of fatigue can be less than or greater than one [36]. A threshold of 0.3% strain allows a comparison of cyclic loading vs impulse loading [29].

In contrast to the previous analysis from Bray and Travasarou [32] that did not register damage, Table 4 and Figure 6 show that when being modified from cyclic loading to impulse loading, the damage rate changes at varying stress levels. These results identify degradation to the soil structure that might not be seen immediately but overtime can cause failure if left unchecked. This level of damage can be catastrophic in infrastructure that is constructed to a certain level based on the existing seismic design criteria. Using this method, the data identifies the potential failure from settlement due to earthquake swarms and should be considered in seismic evaluations.

5. Conclusion

Induced seismicity or induced earthquakes have become of great concern in recent years as rates of these events continue to grow. The inducement of seismicity from underground and surface mining, extraction of oil and gas, reservoir impoundments, and injection of fluids into geologic formations at the subsurface has been understood for some time now; however, these studies neglect incorporating the potential effects that these impulse loads may have on civil engineering systems. One of these potential effects is soil fatigue which can be considered a slow weakening of material because of sources external to the structure that act upon the reliability of it. This should be considered in current evaluation standards and studied to determine if the structure can sustain impulse loading that occurs at shallow depths to identify issues with the foundation prior to failure.

The introduction of a new damage equation is an extension of the Allotey and Naggers [35] model that modifies the loading criteria to impulse in lieu of cyclic to get a better depiction of soil degradation from induced seismic events. It was further modified to include a nonlinear function with loading cycles that is a stress dependent variable for both applied stress and confining pressure. The limitation of the Allotey and Nagger [35] model to determine soil degradation from induced seismic events was based on cyclic loads which do not depict strains that develop from impulse loads. Based on the reformulation of the equation, a better picture of potential damage effects to soils near the surface under impulse loading can be attained. This redundancy is needed as the existing process to access damage to infrastructure from induced seismicity is not adequate as it requires a better understanding of the failure modes and threshold limits within the Seismic Hazard and vulnerabilities structures that are not well equipped to survive seismic loading. Moreover, the difficulty in quantifying the seismic hazard for induced event continues as the hazard is not completely understood and changes in geoengineered locations, activities, and technologies are ever present. However, thorough innovative processes and further studies on this particular topic will allow for a better assessment and determination of detrimental degradation to be observed at the subsurface.

Data Availability

All data used to support the findings of this study can be obtained via the published references.

Conflicts of Interest

The authors declare that they have no conflicts of interest.

Acknowledgments

The authors would like to acknowledge M.D. Antwine, W.W. Berry, A.L. Cunningham, W.R. Rowland, and K.E. Winters of the US Army Engineer Research and Development Center for their assistance in experimental execution. The laboratory research was funded through the US Army, Acquisition, Logistics and Technology (ASAALT) and US Army Corps of Engineers.

References

[1] M. E. Harr, *Reliability Based Design in Civil Engineering*, Dover Publications, Inc., New York, NY, USA, 1996.

[2] O.-D. S. Taylor, A. P. Lester, and T. A. Lee, "Hazard and risk potential of unconventional hydrocarbon development-induced seismicity within the central United States," *Natural Hazards Review*, vol. 16, no. 4, 2015.

[3] O.-D. S. Taylor, A. P. Lester, and T. A. Lee, "Unconventional hydrocarbon development hazards within the central United

States: report 1, overview and potential risk to infrastructure," Technical report ERDC/GSL TR-15-26, US Army Engineer Research and Development Center, Vicksburg, MS, USA, 2015.

[4] O.-D. S. Taylor, A. Lester III, T. A. Lee, and M. H. McKenna, "Can small magnitude induced seismic events actually cause damage?" *Natural Hazards Challenges in Civil Engineering*, vol. 2018, Article ID 2056123, 5 pages, 2018.

[5] I. M. Idriss and R. W. Boulanger, *Soil Liquefaction during Earthquakes*, p. 237, Earthquake Engineering Research Institute, University of California, Davis, CA, USA, 2008.

[6] H. Seed and I. I. M. Bolton, "A simplified procedure for evaluating soil liquefaction potential," in *Earthquake Engineering Research Center, Report No. EERC-70-9*, University of California, Berkley, CA, USA, 1970.

[7] E. Eseller-Bayat, M. K. Yegian, A. Alshawabkeh, and S. Gokyer, "Liquefaction response of partially saturated sands I: experimental results," *Journal of Geotechnical and Geoenvironmental Engineering*, vol. 139, no. 6, pp. 863–871, 2013.

[8] M. Okamura and Y. Soga, "Effects of pore fluid compressibility on liquefaction resistance of partially saturated sand," *Soils and Foundations*, vol. 46, no. 5, pp. 695–700, 2006.

[9] P. Folger and M. Tiemann, *Human-Induced Earthquakes from Deep-Well Injection: A Brief Overview*, Congressional Research Service, Washington, DC, USA, 2016.

[10] J. L. Mahani, "Myths and facts wastewater injection, hydraulic fracturing, enhanced oil recovery, and induced seismicity," *Seismological Research Letters*, vol. 86, no. 4, pp. 1060–1067, 2015.

[11] G. Atkinson, K. Assatourians, B. Cheadle, and W. Greig, "Ground motions from three recent earthquakes in Western Alberta and Northeastern British Columbia and their implications for induced-seismicity hazard in eastern regions," *Seismological Research Letters*, vol. 86, no. 3, pp. 1022–1031, 2015.

[12] K. M. Keranen, H. M. Savage, G. A. Abers, and E. S. Cochran, *Potentially Induced Earthquakes in Oklahoma, USA: Links between Wastewater Injection and the 2011 M 5.7 Earthquake Sequence*, Geological Society of America, Boulder, CO, USA, 2013.

[13] A. Kuchment, "Drilling for earthquakes," *Scientific American*, vol. 315, no. 1, pp. 46–53, 2016.

[14] T. Candela, B. Wassing, J. T. Heege, and L. Buijze, "How earthquakes are induced," *Science*, vol. 360, no. 6389, pp. 598–600, 2018.

[15] N. J. Van der Elst, M. T. Page, D. A. Weiser, T. H. W. Goebel, and S. M. Hosseini, "Induced earthquake magnitudes are as large as (statistically) expected," *Journal of Geophysical Research: Solid Earth*, vol. 121, no. 6, pp. 4575–4590, 2016.

[16] M. Galis, J. P. Ampuero, P. M. Mai, and F. Cappa, "Induced seismicity provides insight into why earthquake ruptures stop," *Science Advances*, vol. 3, no. 12, Article ID eaap7528, 2017.

[17] G. Zalachoris and E. M. Rathje, "Ground motion model for small-to-moderate earthquakes in Texas, Oklahoma, and Kansas," *Earthquake Spectra*, vol. 35, no. 1, pp. 1–20, 2019.

[18] F. Khosravikia, P. Clayton, and Z. Nagy, "Artificial neural network-based framework for developing ground-motion models for natrual and induced earthquakes in Oklahoma, Kansas, and Texas," *Seismological Research Letters*, vol. 90, no. 2, pp. 604–613, 2019.

[19] L. Quinones, H. R. DeShon, S. Jeong et al., "Tracking induced seismicity in the Fort worth basin: a summary of the 2008–2018 north Texas earthquake study catalog," *Bulletin of the Seismological Society of America*, vol. 109, no. 4, pp. 1203–1216, 2019.

[20] J. I. Walter, C. Frohlich, and T. Borgfeldt, "Natural and induced seismicity in the Texas and Oklahoma panhandles," *Seismological Research Letters*, vol. 89, no. 6, pp. 2437–2446, 2018.

[21] M. Barba-Sevilla, B. Baird, A. Liel, and K. Tiampo, "Hazard implications of the 2016 Mw 5.0 cushing, OK earthquake from a joint analysis of damage and InSAR data," *Remote Sensing*, vol. 10, no. 11, p. 1715, 2018.

[22] R. E. Chase, A. B. Liel, N. Luco, and B. W. Baird, "Seismic loss and damage in light-frame wood buildings from sequences of induced seismicity," *Earthquake Engineering and Structural Dynamics*, vol. 48, no. 12, pp. 1365–1383, 2019.

[23] F. Khosravikia, A. Potter, and V. Prakhov, *Seismic Vulnerability and Post-event Actions for Texas Bridge Infrastructure," FHWA/TX-18/0-6916-1*, Center for Transportation Research, Austin, TX, USA, 2018.

[24] F. Khosravikia, J. Kurkowski, and P. Clayton, "Fragility of masonry veneers to human-induced Central US earthquakes using neural network models," *Journal of Building Engineering*, vol. 28, Article ID 101100, 2020.

[25] T. Liu, N. Luco, and A. B. Liel, "Increases in life-safety risks to building occupants from induced earthquakes in the Central United States," *Earthquake Spectra*, vol. 35, no. 2, pp. 471–488, 2019.

[26] O.-D. S. Taylor, A. L. Cunningham, K. E. Martin, R. E. Walker, M. H. McKenna, and P. G. Kinnebrew, "Near-surface soils: ultrasonic near-surface inundation testing," *Near Surface Geophysics*, vol. 17, no. 4, pp. 331–344, 2019.

[27] O.-D. S. Taylor, K. E. Winters, W. W. Berry, L. A. Walshire, and P. G. Kinnebrew, "Near-surface soils: self-supported unconfined drained sand specimens," *Canadian Geotechnical Journal*, vol. 56, no. 3, pp. 307–319, 2019.

[28] O.-D. S. Taylor, K. E. Winters, W. W. Berry, and M. L. Zuzulock, "Dynamic failure potential of partially saturated sand under ultra-low confining pressures," in *Proceedings of Geotechnical Earthquake Engineering and Soil Dynamics*, Austin, TX, USA, June 2017.

[29] O.-D. S. Taylor, *Use of an Energy-Based Liquefaction Approach to Predict Deformation in Silts Due to Pile Driving*, University of Rhode Island, South Kingstown, RI, USA, 2011.

[30] N. M. Newmark, "Effects of earthquakes on dams and embankments," *Géotechnique*, vol. 15, no. 2, pp. 139–160, 1965.

[31] H. B. Seed, "Considerations in the earthquake-resistant design of earth and rockfill dams," *Geotechnique*, vol. 29, no. 3, 1979.

[32] J. D. Bray and T. Travasarou, "Simplified procedure for estimating earthquake-induced deviatoric slope displacements," *Journal of Geotechnical and Geoenvironmental Engineering*, vol. 133, no. 4, pp. 381–392, 2007.

[33] J. D. Bray and T. Travasarou, "Pseudostatic slope stability procedure," in *Proceedings of the 5th International Conference on Earthquake Geotechnical Engineering*, pp. 10–13, Santiago, Chile, 2011.

[34] R. W. Jibson, E. M. Rathje, M. W. Jibson, and Y. W. Lee, *SLAMMER—Seismic Landslide Movement Modeled Using Earthquake Records*, US Geological Survey Techniques and Methods, Reston, VA, USA, 2014.

[35] N. Allotey and M. H. El Naggar, "A consistent soil fatigue framework based on the number of equivalent cycles," *Geotechnical and Geological Engineering*, vol. 26, no. 1, pp. 65–77, 2008.

[36] W. V. Paepegem and J. Degrieck, "Effects of load sequence and block loading on the fatigue response of fiber-reinforced composites," *Mechanics of Advanced Materials and Structures*, vol. 9, no. 1, pp. 19–35, 2002.